CHAPTER 167

IRREGULAR WAVE LOADING ON A CONICAL STRUCTURE

Wayne W. Jamieson, Etienne P.D. Mansard and
Geoffrey R. Mogridge[1]

ABSTRACT

        The horizontal forces, vertical forces and over-
turning moments exerted by waves on a fixed model of a 45°
conical structure are presented. Irregular wave loading
tests were conducted for a range of conditions described by
base diameter on peak period wave length D/L_p from 0.31
to 1.76, water depth on peak period wave length h/L_p from
0.11 to 0.63, and significant wave height on peak period
wave length H_{m_0}/L_p up to 0.07.

        Time series records, spectral densities and
transfer functions for the irregular wave loading tests are
used to illustrate the nonlinear nature of the measured
wave loads. In most cases, similar trends in wave loading
were observed for irregular and regular wave tests. For
deep-water waves, the irregular and regular force measure-
ments showed spectral peaks at the second harmonic of the
wave frequency even though the waves themselves had rela-
tively small second-order components. However, unlike the
regular wave loading results, the fundamental spectral peak
frequency for the irregular wave forces occurred at a fre-
quency considerably lower than the peak frequency of the
waves. Although linear diffraction theory provided a rea-
sonable estimate of the wave forces for waves of low steep-
ness, larger deviations were often present for higher wave
steepness results. Comparison of theory and experiment for
overturning moments was generally very poor for most wave
conditions.

INTRODUCTION

        In recent years numerous designs of offshore
structures for drilling and production have been proposed
for use in arctic regions. Buslov and Krahl (1983) have
described sixty-one conceptual designs for arctic offshore
platforms, some of which are currently being constructed,
others of which are operational. Some of the designs in-
corporate large bottom-founded conical-shaped structures

---

[1] Research Officers, National Research Council of Canada,
   Hydraulics Laboratory, Montreal Rd., Bldg. M-32, Ottawa,
   Ontario, K1A 0R6, Canada.

which cause ice sheets to fail predominantly by bending
rather than by buckling or crushing, in order to reduce ice
loading. Of course, the relatively small area subjected to
ice loading near the water surface also minimizes ice
forces. The large hull of this type of gravity structure
provides resistance against sliding and overturning at its
base, but also provides sufficient buoyancy when deballas-
ted so that it can be towed while floating on its hull to
another site. Although none of these conical structures
have yet been built, they are currently being considered
for use in a range of water depths between 10 m and 80 m.

        The wave loading on some of these proposed coni-
cal structures has been modelled both physically and numer-
ically, but the results are for the most part proprietary
and as a result, published data is very limited. Isaacson
(1982) has published some results of numerical calculations
for the case of a surface-piercing 45° conical structure
utilizing the body's vertical axisymmetry to reduce consi-
derably the computational effort required for bodies of
arbitrary shape. Jamieson et al. (1985) have carried out
regular wave loading measurements on a model of a surface-
piercing 45° conical structure. The model was a simple
axisymmetric structure which somewhat characterized the
shape of proposed prototype conical structures, could
easily be modelled both physically and mathematically and
the results could be published without infringing on any
proprietary designs. The tests indicated extremely nonlin-
ear wave loading resulting in considerable differences
between experiment and linear diffraction theory particu-
larly for higher steepness waves. In this paper, the hori-
zontal forces, vertical forces and overturning moments
exerted by irregular waves on the same 45° conical model
are presented. The irregular wave loading results are com-
pared to those measured for regular waves and those compu-
ted by linear diffraction theory.

EXPERIMENTAL SETUP

        Figure 1 shows a photograph of the conical
model. It was constructed of 6 mm thick plexiglass in the
shape of a 45° right circular cone, 125.5 cm in diameter at
the base (see Figure 2). The model was tested in a water
depth of 44.6 cm. Assuming a scale of approximately 1:100,
the model corresponds to a full scale 45° conical gravity
platform with a 126 m diameter at the base, resting in a
water depth of 45 m. Model dimensions will be used
throughout this paper. For structural considerations, the
base of the model was slightly rounded rather than sharp-
edged. Figures 3 and 4 show a photograph and schematic
views respectively of the wave flume and the experimental
setup. The model was installed 11 m from the wave genera-
tor in the centre of the 13 m wide portion of the wave
flume. The outer circumference of the model base was
sealed and the underside of the model was vented to atmos-
pheric pressure so that no dynamic wave pressures were
experienced underneath the model. This condition allowed
the measurement of wave loading due to fluid pressures on
the upper surfaces of the model, which is all that is of
interest in the present study, because under full scale
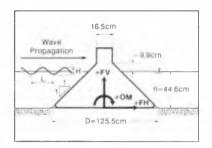
Figure 1. Model of Conical Structure

Figure 2. Model Dimensions and Sign Convention for Wave Loads

Figure 3. Photograph of Wave Flume and Experimental Setup

Side channel
(1m wide)

Wave probe

Upright wave absorber

Conical model

Stone
beach
(1:15)

13m

Wave generator

Upright wave absorber

Inside of wave flume wall

(a) Plan View

Upright wave absorber
(5 rows of perforated sheets)

Wave generator
(piston mode)

Conical
model

Stone beach

80cm

SWL

60cm

Load cells

3m — 11m — 5m — 9m

28m

(b) Side View

Upright wave absorber
(3 rows of perforated sheets)

Interior wall
(6mm thick steel plate)

Side channel

Conical
model

Wave probe

SWL

44.6cm

0.9m

0.9m
1.0m

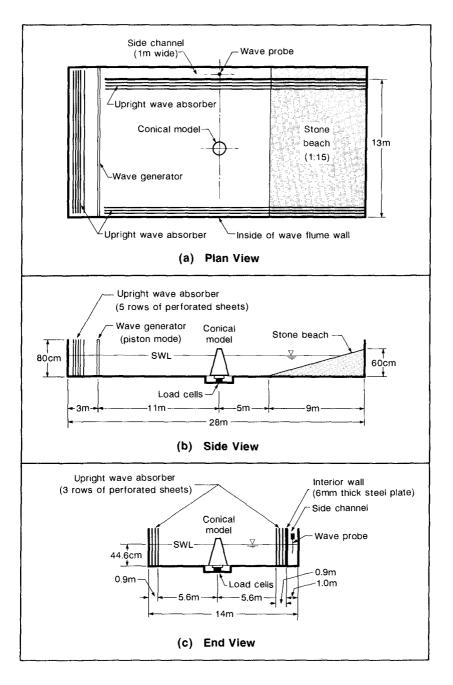Load cells

5.6m — 5.6m

14m

(c) End View

Figure 4. Schematic of Wave Flume and Experimental Setup

conditions the wave pressures underneath the structure propagate through a porous foundation rather than through an open gap as in a model study.

The base of the model was mounted to a three-component load cell dynamometer system which was in turn bolted to the bottom of a circular pit located below the concrete floor of the wave flume. The dynamometer system was designed so that three individual load cells could be bolted together in a configuration which allowed the measurement of horizontal force (FH), vertical force (FV) and overturning moment (OM). The three load cells were constructed of steel and designed by the Hydraulics Laboratory to have a very high stiffness-sensitivity product with only small cross-coupling errors. Each of the load cells used semiconductor strain gauges, which were thermally compensated and thoroughly waterproofed to minimize environmental problems caused by temperature changes and high humidity. They were initially calibrated individually in air on a calibration rig. Combined nonrepeatability, nonlinearity and hysteresis of the load cells were less than ±0.5%. During the testing program, the load cell calibrations were checked once a day by applying known loads to the model by means of a system of low-friction pulleys. Natural frequencies of vibration of the total system were measured by applying a step load to the model in both vertical and horizontal directions, and recording the voltage outputs from each load cell sampled at a rate of 500 samples/ second. With 44.6 cm of water in the wave flume, the natural frequencies of vibration were 30 Hz, 13 Hz and 30 Hz as measured by the horizontal and vertical force load cells, and the torque load cell, respectively.

In this paper, the measured wave forces and overturning moments on the conical model have been related to the incident wave conditions, that is, the waves that occur at the location of the model with the model removed. To eliminate the time required to regenerate the waves with the model removed, all incident waves were measured by a capacitive wire wave probe located alongside the conical model in the 1 m wide side channel (see Figures 3 and 4). The side channel was separated from the main channel by a 6 mm thick solid steel plate wall.

Voltage signals from the test instrumentation went to a high-speed data acquisition package consisting of programmable-gain differential amplifiers, a high-speed solid-state multiplexer and an analog-to-digital converter. The output from the wave probe required no amplification; however, the two force load cell signals and the torque load cell output were amplified 200 times. A minicomputer was used for the acquisition, processing, plotting and storage of experimental data.

The waves generated by the wave machine moved along the length of the flume past the model and were effectively absorbed by the 1 in 15 sloped stone beach at the end of the flume shown in Figure 4. Wave reflection coefficients (ratio of reflected wave height to incident wave height expressed as a percentage) for this beach were less than 5% for all wave conditions tested.

          Figures 3 and 4 show the placement of upright
wave absorbers along the side walls of the 13 m wide main
channel.   Each of these side absorbers consisted of three
rows of perforated vertical sheets placed over a distance
of 90 cm.   The porosity of the rows of sheets decreased
towards the rear of each absorber.   The design is based on
a new type of efficient upright wave absorber developed at
the Hydraulics Laboratory of the National Research Council
of Canada (Jamieson and Mansard (1987)).   It is particular-
ly suitable for laboratory wave basins where (1) limited
space is available for the installation of absorbers, (2)
testing at variable water depths is essential without hav-
ing to make adjustments to the absorber, and (3) reflected
wave energy from the absorber must be minimized for a wide
range of water depths, wave heights and wave periods (wave
reflection coefficients of less than 5%).   The placement of
the rows of perforated sheets in the side absorbers is such
that the waves generated from the wavemaker moved along the
length of the flume through the side absorbers quite freely
but the waves radiated off the conical model were effec-
tively absorbed.   The attenuation of the waves as they pro-
pagated in the main channel was negligible, so that the
side channel wave probe effectively measured the incident
wave heights.   After a test, the waves in the flume were
attenuated in less than 5 minutes compared to a settling
down period of more than 30 minutes if only solid side
walls were used.   An upright wave absorber was also used to
provide effective wave absorption over a distance of 1.5 m
between the rear of the wave generator and the back wall of
the wave flume.

EXPERIMENTAL METHOD

          The irregular waves generated in this study were
synthesized using the random phase spectrum method.   It is
a technique which pairs the amplitude spectrum derived from
a given target spectral density with a randomly selected
phase spectrum, and creates a time series by inverse
Fourier transformation (Funke and Mansard (1984)).   JONSWAP
spectral densities with a peak enhancement factor γ = 3.3
were used as target spectra.   Each time series was synthe-
sized with a record length of 300 s, resulting in approxi-
mately 150 waves for the lowest spectral frequency and
about 450 waves for the highest.

          A number of sea states with different spectral
peak frequencies (f_p = 0.48, 0.69, 0.80, 0.95, 1.02,
1.16, 1.33 and 1.48 Hz) were generated.   For each peak fre-
quency, the significant wave height H_{mo} of the sea state
was varied in order to evaluate the influence of nonlinear-
ities due to wave steepness.   This was achieved by rescal-
ing the time series to match the desired variance.   A mini-
mum of four significant wave heights having wave steep-
nesses (H_{mo}/L_p) between 0.01 and 0.07 were run for each
spectral peak frequency listed above.   Since only the vari-
ance of the sea state was changed, other parameters such as
groupiness factor, ratio of maximum to significant wave
heights etc. were kept constant.

          Sampling of the data was commenced three minutes
after the first waves had passed the model.   For each irre-

gular wave test, the incident wave profile in the side
channel and the wave loads (FH, FV and OM) were sampled at
a rate of 10 samples per second, for a total record length
of 300 seconds. The water depth was maintained at 44.6 cm
throughout the entire testing program. Total forces and
overturning moments about the base of the model (see
Figure 2) were computed and plotted along with the incident
wave profile measured in the side channel.

Spectral analysis of the wave loads and the inci-
dent wave record was carried out for each test. The spec-
tral analysis used in this study is an algorithm which per-
forms a Fourier transform over the entire record length and
computes the spectral ordinates by squaring and summing the
complex Fourier coefficients. Smoothing of the spectrum
was carried out by averaging the adjacent spectral esti-
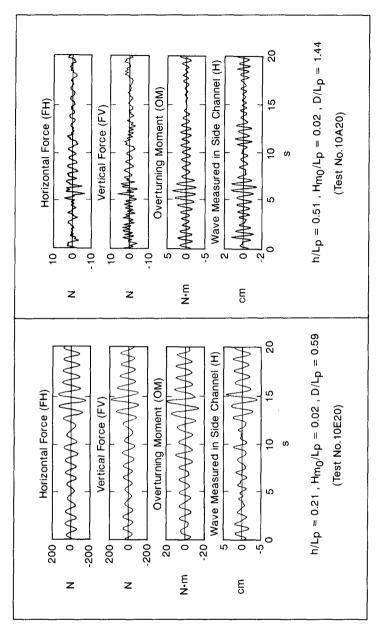mates using a rectangular window.

Transfer functions of the irregular wave loads
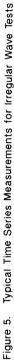were calculated for each test as follows:

$$TRF(f) = [S_{WL}(f) \ / \ S_{IW}(f)]^{\frac{1}{2}}$$

where
$TRF(f)$ = Transfer function of the wave load (FH, FV or OM)
$S_{WL}(f)$ = Spectral density of the corresponding wave load
$S_{IW}(f)$ = Spectral density of the incident wave (H).

Regular wave tests were carried out for the pur-
pose of comparison with the irregular wave tests. Samp-
ling of the data was commenced after ten waves had passed
the model. For each regular wave test, the incident wave
profile and the wave loads were sampled at a rate of 100
samples per second for a total record length of 50 s.
Regular waves were generated for a wide range of frequen-
cies (f = 0.48, 0.60, 0.69, 0.80, 0.88, 0.95, 1.02, 1.16,
1.33 and 1.48 Hz). A minimum of six wave heights having
wave steepnesses (H/L) between 0.01 and 0.10 were generated
for each wave frequency listed above.

EXPERIMENTAL RESULTS AND DISCUSSION

Time Series of Wave Loading

Figure 5 shows typical time series measurements
of horizontal force (FH), vertical force (FV), overturning
moment (OM) and the incident wave measured in the side
channel (H) for two irregular wave tests of low wave steep-
ness (H_{m_0}/L_p = 0.02). The time series results shown
are representative of the tests carried out for interme-
diate-water depths (h/L_p = 0.21) and deep-water depths
(h/L_p = 0.51). Only a 20 s portion of the 300 s record
length is shown for each of the tests. The time series of
the wave loading results for the intermediate-water depth
(h/L_p = 0.21) results are smooth and one would expect the
spectral analysis of the wave loading to give the same peak
frequency as the waves. For the deep-water results (h/L_p
= 0.51), a similar observation is evident for the overturn-
ing moment (OM). However, for the force records (FH and
FV) both high and low frequency components are evident
which are not identifiable in the wave record. Spectral

Figure 5.   Typical Time Series Measurements for Irregular Wave Tests

analysis results of the data is discussed in the next section.

Spectral Densities of Wave Loading

Spectral density measurements for irregular and regular wave tests for a relative depth of 0.21 are shown in Figure 6. This illustrates the type of irregular wave loading commonly observed for intermediate-water depths, i.e. the peak frequency (0.80 Hz) of the wave forces (FH and FV) and the overturning moment (OM) is the same as that of the waves. In the time series for this test (shown in Figure 5) it can be seen that the frequency of the wave loads and the waves is about the same. The spectral density results for the regular wave test in Figure 6 also shows that for an intermediate-water depth, h/L = 0.21, the peak frequency of the wave loads coincides with that of the waves. The above examples are for low steepness waves for irregular and regular wave trains; the same general results occur for higher steepness waves.

Spectral density measurements for irregular and regular wave loading for deep-water waves (a relative depth of 0.51) in Figure 7 show the emergence of strong nonlinearities in the forces which are not present in the incident wave spectrum. The results for the regular wave test in Figure 7 are similar to those published previously for regular waves by Jamieson et al. (1985). For the horizontal and vertical forces, the spectral density plots show very little response at the fundamental frequency (1.34 Hz) of the incident waves; most of the response is at the second harmonic (2.68 Hz). Thus, it is not surprising that the irregular deep-water wave test (f_p = 1.30 Hz) results illustrated in Figure 7 indicate significant response in the spectra for the horizontal and vertical forces at frequencies approximately twice the peak frequency of the waves (2.60 Hz). However, it is not clear why the horizontal and vertical force spectral peaks for this irregular test do not occur at the same peak frequency as the waves (1.30 Hz) but at the slightly lower frequency of 1.04 Hz. It is not known why this occurs. Even though the magnitude of the wave loads for these conditions is quite small, it may still be important to understand the reason for this unusual nonlinear transfer of response. The regular wave loading results reported by Jamieson et al. (1985) for horizontal and vertical force, as well as the regular wave force results shown in Figure 7, do not show a similar shift of response because there is no interaction between frequency components. Indications of these two phenomena have already been observed in the time series plots (Figure 5). For the test results shown in Figure 7, the spectral peaks for the overturning moments occur at the same peak frequencies as the waves (1.30 Hz and 1.34 Hz for the irre- under other wave conditions a significant amount of energy in the spectra for the overturning moment was measured at frequencies approximately twice the peak frequency of the waves.

In the previous paper by Jamieson et al. (1985) it was observed that for regular deep-water waves, the wave
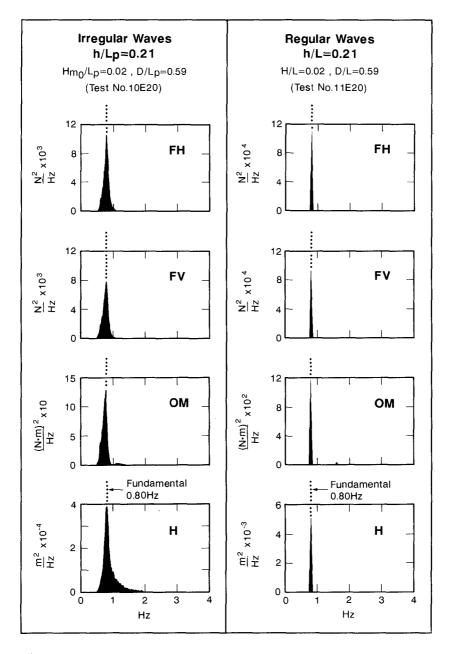
Figure 6.   Typical Spectral Density Measurements for a Relative Depth of 0.21
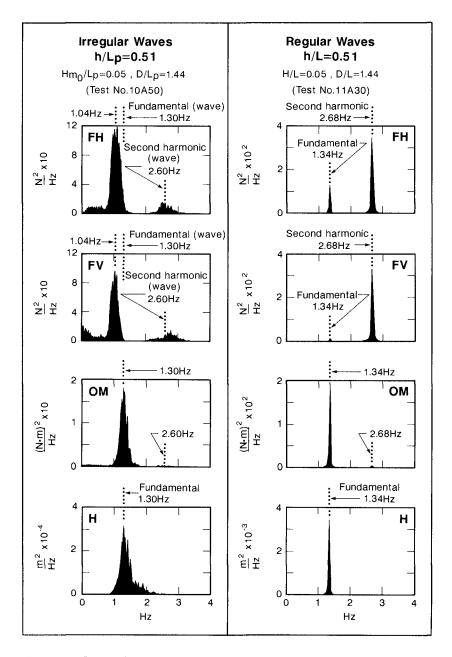
Figure 7. Typical Spectral Density Measurements for a Relative Depth of 0.51

loading was predominantly at the second-harmonic frequency
of the waves (particularly for the horizontal and vertical
wave forces). In that paper there was a brief discussion
of previous reportings of second-order pressure fluctua-
tions which do not attenuate with water depth, i.e.
Longuet-Higgins (1950), Rundgren (1958), Hogben and
Standing (1975). In the paper by Jamieson et al. (1985),
it was observed that in addition to the wave frequency, the
structural shape is important in determining whether
second-harmonic forces and moments will appear. Thus, for
a conical shape, the increasing diameter of the structure
towards the bottom results in an increasing influence of
the second-harmonic pressures where they are larger rela-
tive to the linear pressures. As far as the authors are
aware, the shift in the irregular wave loading spectral
peaks to a frequency lower than the wave excitation spec-
tral peak frequency, has not been observed before.

Wave Load Transfer Functions

        Transfer functions for horizontal force (FH),
vertical force (FV) and overturning moment (OM) are plotted
in Figure 8 for irregular wave tests having wave steep-
nesses, H_{m0}/L_p = 0.02 and 0.06. Each of these transfer
functions has only been calculated and plotted over the
range of frequencies where there is significant energy in
the incident wave spectrum for the given irregular wave
test. Thus the nonlinear transfer of response in the wave
loads from the wave frequency to lower or higher frequen-
cies is not evident in the plotted results (shown in Figure
8) because the data has been truncated. The linear trans-
fer function used here has large errors at frequencies
where the energy of the wave excitation is small or negli-
gible.

        Transfer functions for eight tests with peak wave
frequencies (as outlined in the experimental method) rang-
ing from 0.48 Hz to 1.48 Hz each with a wave steepness of
H_{m0}/L_p = 0.02 have been plotted on the left side of
Figure 8 for each wave load (FH, FV and OM). For these low
wave steepness results, all of the transfer functions fall
on the same curve for each of the wave loads.

        Transfer functions for seven tests with peak wave
frequencies (as outlined in the experimental method) rang-
ing from 0.69 Hz to 1.48 Hz each with a wave steepness of
H_{m0}/L_p = 0.06 have been plotted on the right side of
Figure 8 for the wave loads. For these higher steepness
results, the transfer functions did not all fall on the
same curves but showed some scatter as indicated by the
wider lines used in plotting the curves. This is particu-
larly evident for the plotted transfer functions of hori-
zontal force and overturning moment.

        If the wave loading results were linear, then the
transfer functions would be the same for all wave steepness
results. However, the results for the two wave steepnesses
(H_{m0}/L_p = 0.02 and 0.06) in Figure 8 show a noticeable
difference between the transfer functions for the different
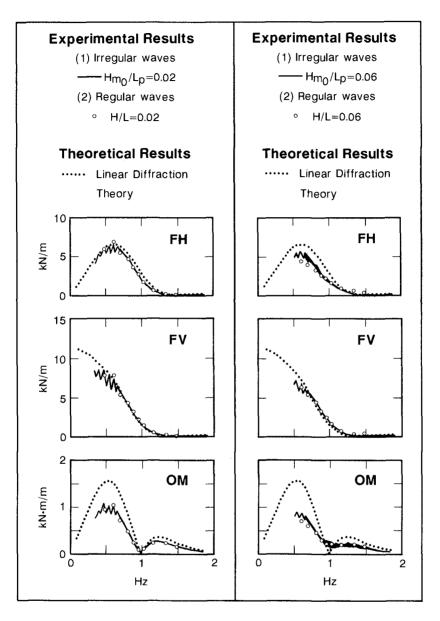wave steepnesses. Although not shown here, the transfer

Figure 8.   Comparison Between Experimental and Theoretical
Wave Load Transfer Functions

functions for the other wave steepness results that were
tested were also plotted and showed the same trends which
are apparent in Figure 8. The variations in the transfer
functions clearly indicate that the interaction between the
conical structure and the incident waves is nonlinear.

Regular wave loading results are also included in
Figure 8. Response amplitude operators (RAOs) were calcu-
lated for the regular wave tests previously described in
the experimental method and are plotted for wave steep-
nesses H/L = 0.02 and 0.06. The RAOs were calculated by
adding the maximum positive wave load to the maximum nega-
tive wave load (since the absolute magnitudes were general-
ly not equal) and dividing by the incident wave height.
The RAOs for the regular waves are in good agreement with
the transfer functions calculated for the irregular waves
for all the wave loading conditions that were tested.

The theoretical wave load transfer functions
shown in Figure 8 were calculated using the linear wave
diffraction program (NPLWAVE) described by Hogben and
Standing (1975). The lowest wave steepness results provi-
ded the closest agreement between theory and experiment,
while the largest deviations between theory and experiment
were measured for the highest wave steepness results. The
transfer functions for vertical forces indicate very good
agreement between linear diffraction theory and experiment
for a wide range of frequencies and wave steepnesses.
Extremely poor agreement between theory and experiment
exists for the overturning moments. Other than in the
vicinity of 1 Hz, the linear diffraction theory usually
overestimates the measured overturning moments by more than
50%. For low steepness waves (H_{m_0}/L_p = 0.02), linear
diffraction theory slightly overestimates most of the hori-
zontal force measurements; however, for higher steepness
waves (H_{m_0}/L_p = 0.06) such as those shown in Figure 8,
the theory generally overestimates the measured results by
more than 40%. For higher frequency results, the theoreti-
cal and experimental results are very similar although in
this range of frequencies the wave forces are very small in
magnitude compared to the higher loads measured for the
lower frequency measurements.

CONCLUSIONS

1.   Horizontal forces, vertical forces and overturning
     moments exerted by waves on a model of a surface-
     piercing 45° right circular conical structure have
     been measured.
2.   Time series records, spectral densities and transfer
     functions for irregular wave loading tests have illus-
     trated the nonlinear nature of the measured wave
     loads.
3.   Similar trends in wave loading have been observed for
     irregular and regular wave tests.
4.   For deep-water waves, the irregular and regular force
     measurements have shown spectral peaks at the second
     harmonic of the wave frequency even though the waves
     themselves had negligibly small second-order
     components. However, unlike the regular wave loading

results, the fundamental for the irregular wave forces occurs at a frequency considerably lower than the peak frequency of the waves.

5. Linear diffraction theory provides reasonable esti-mates of the wave forces for waves of low steepness; however, large deviations occur for waves of higher steepness. Linear diffraction theory generally pro-vides very poor estimates of the overturning moments. Presently there is not a theoretical nonlinear method that provides an accurate solution of the wave loading on conical structures; thus, the overall wave loading must be determined by physical model tests.

REFERENCES

Buslov, V.M. and N.W. Krahl. (1983). "Fifty-one New Con-cepts for Arctic Drilling and Production", Ocean Industry, Vol. 18 (1983), Parts 1, 2 and 3, Vol. 19 (1984), Parts 4, 5 and 6, 16 pp.

Funke, E.R. and E.P.D. Mansard. (1984). "The NRCC 'Random' Wave Generation Package", National Research Council of Canada, Hydraulics Laboratory Technical Report, TR-HY-002.

Hogben, N. and R.G. Standing. (1975). "Wave Loads on Large Bodies", International Symposium on the Dynamics of Marine Vehicles and Structures in Waves, edited by R.E.D. Bishop and W.G. Price, Mechanical Engineering Publications Limited, London, pp. 258-277, Authors' Replies, pp. 439-441.

Isaacson, M. de St. Q. (1982). "Fixed and Floating Axisymmetric Structures in Waves", Proc. ASCE, Vol. 18, No. WW2, May, pp. 180-199.

Jamieson, W.W., E.P.D. Mansard and G.R. Mogridge. (1985). "Wave Loading on a Conical Gravity Platform", Proc. 4th International Conference on Behaviour of Offshore Structures, Delft, The Netherlands, July, pp. 673-684.

Jamieson, W.W. and E.P.D. Mansard. (1987). "An Efficient Upright Wave Absorber", ASCE Specialty Conference on Coastal Hydrodynamics, University of Delaware, Newark, Delaware, June 29-July 1, pp. 124-139.

Longuet-Higgins, M.S. (1950). "A Theory of the Origin of Microseisms", Philosophical Transactions of the Royal Society of London, Series A, Vol. 243, No. 857, September, pp. 1-35.

Rundgren, L. (1958). "Water Wave Forces: A Theoretical and Laboratory Study", Transactions of the Royal Institute of Technology, Stockholm, Sweden, Bulletin No. 54 of the Institution of Hydraulics, 123 pp.

NRCC, Hydraulics Laboratory Technical Reports are available upon request from the Hydraulics Laboratory, Bldg. M-32, National Research Council of Canada, Montreal Road, Ottawa, Ontario, K1A 0R6, Canada.